Science Translational Medicine
AAAS

Vaccine-Induced Anti-HA2 Antibodies Promote Virus Fusion and Enhance Influenza Virus Respiratory Disease

Surender Khurana *et al.*

Sci Transl Med **5**, 200ra114 (2013);
DOI: 10.1126/scitranslmed.3006366

Editor's Summary

The (Mis)match Game

Even the most beneficial things––like vaccines––sometimes have a downside. Learning what causes the downside is critical for avoiding it. In the case of viral vaccines, there have been some reports of rare vaccine-induced disease enhancement ––for example, vaccine-associated enhanced respiratory disease (VAERD) for influenza. Khurana *et al.* now report that mismatched strains of the same subtype of influenza may lead to VAERD in pigs.

The authors vaccinated pigs with whole inactivated H1N2 influenza virus. These pigs had enhanced pneumonia and disease after infection with another strain ––pH1N1. Looking more closely, the authors found that the immune sera from the H1N2-vaccinated pigs contained high titers of cross-reactive hemagglutinin antibodies. These antibodies actually enhanced pH1N1 infection in cell culture by promoting virus membrane fusion activity, and this enhanced fusion correlated with lung pathology. This mechanism of VAERD should be considered when devising strategies to devise a universal flu vaccine.

Science Translational Medicine (print ISSN 1946-6234; online ISSN 1946-6242) is published weekly, except the last week in December, by the American Association for the Advancement of Science, 1200 New York Avenue NW, Washington, DC 20005.

INFLUENZA

Vaccine-Induced Anti-HA2 Antibodies Promote Virus Fusion and Enhance Influenza Virus Respiratory Disease

Surender Khurana,[1] Crystal L. Loving,[2] Jody Manischewitz,[1] Lisa R. King,[1] Phillip C. Gauger,[3] Jamie Henningson,[4] Amy L. Vincent,[2]* Hana Golding[1]*

Vaccine-induced disease enhancement has been described in connection with several viral vaccines in animal models and in humans. We investigated a swine model to evaluate mismatched influenza vaccine-associated enhanced respiratory disease (VAERD) after pH1N1 infection. Vaccinating pigs with whole inactivated H1N2 (human-like) virus vaccine (WIV-H1N2) resulted in enhanced pneumonia and disease after pH1N1 infection. WIV-H1N2 immune sera contained high titers of cross-reactive anti-pH1N1 hemagglutinin (HA) antibodies that bound exclusively to the HA2 domain but not to the HA1 globular head. No hemagglutination inhibition titers against pH1N1 (challenge virus) were measured. Epitope mapping using phage display library identified the immunodominant epitope recognized by WIV-H1N2 immune sera as amino acids 32 to 77 of pH1N1-HA2 domain, close to the fusion peptide. These cross-reactive anti-HA2 antibodies enhanced pH1N1 infection of Madin-Darby canine kidney cells by promoting virus membrane fusion activity. The enhanced fusion activity correlated with lung pathology in pigs. This study suggests a role for fusion-enhancing anti-HA2 antibodies in VAERD, in the absence of receptor-blocking virus-neutralizing antibodies. These findings should be considered during the evaluation of universal influenza vaccines designed to elicit HA2 stem-targeting antibodies.

INTRODUCTION

Vaccine-associated enhanced respiratory disease (VAERD) has been reported in multiple respiratory infections in humans and in animals. Seronegative children administered formaldehyde-inactivated respiratory syncytial virus (RSV) vaccine followed by exposure to wild-type RSV demonstrated enhanced respiratory disease (*1*, *2*). Similarly, atypical measles with severe disease was reported in children vaccinated with formalin-inactivated vaccines (*3*). The mechanisms underlying VAERD after respiratory infections are not completely understood and may vary with the disease and/or vaccine modality.

Because the 2009 pH1N1 influenza virus strain was of swine origin, a pig model was used to evaluate the potential of commonly used swine inactivated influenza vaccines to study VAERD when the circulating/infecting influenza strain does not match the vaccine strain. The human-like H1 (δ-cluster) influenza virus is currently endemic in U.S. swine population after introduction of human seasonal H1 influenza virus into swine population (*4*). We previously reported the failure of an inactivated classical swine H1N1 vaccine to protect pigs after infection with an H1N2 swine influenza virus while enhancing the severity of pneumonia (*5*). During the 2009 H1N1 pandemic (pH1N1), further studies demonstrated that pigs vaccinated with whole inactivated virus vaccine containing a human-like H1N2 (WIV-H1N2) and subsequently challenged with pH1N1 had enhanced pneumonia and respiratory disease when compared with nonvaccinated pH1N1-challenged animals, thus providing strong evidence of VAERD after mismatched influenza infection (*6*, *7*).

[1]Division of Viral Products, Center for Biologics Evaluation and Research, U.S. Food and Drug Administration, Bethesda, MD 20892, USA. [2]Virus and Prion Research Unit, National Animal Disease Center, Agricultural Research Service, U.S. Department of Agriculture, Ames, IA 50010, USA. [3]Department of Veterinary Diagnostic and Production Animal Medicine, Ames, IA 50010, USA. [4]Kansas State Veterinary Diagnostic Laboratory, Manhattan, KS 66506, USA.
*Corresponding author. E-mail: hana.golding@fda.hhs.gov (H.G.); Amy.Vincent@ars.usda.gov (A.L.V.)

Here, we used this swine model to investigate the role of vaccination-induced antibody response to gain insight into the mechanisms of VAERD after mismatched pH1N1 influenza virus challenge.

RESULTS

Heterologous inactivated influenza vaccination of pigs results in enhancement of influenza disease after pH1N1 virus challenge

Intratracheal challenge of pigs with the 2009 pandemic H1N1 (A/California/04/2009) virus (pH1N1) 3 weeks after vaccination with whole inactivated H1N2 (A/Swine/Minnesota/02011/08) virus (WIV-H1N2) resulted in VAERD with pronounced macroscopic and microscopic lesions in the lungs (Fig. 1, A and C versus B and D). The percentage of macroscopic and microscopic lesions in the WIV-H1N2–vaccinated animals was threefold higher than in nonvaccinated pigs after pH1N1 challenge (Fig. 1E) and reflected the increased severity of bronchointerstitial pneumonia with necrotizing lymphocytic cuffing accompanied by hemorrhage and interlobular alveolar edema (Fig. 1, B and D).

WIV-H1N2 vaccination generated nonneutralizing binding antibodies against pH1N1 virus that showed high titers of anti–pH1N1-HA2, but not anti-HA1, cross-reactive antibodies

The immune response elicited by WIV-H1N2 vaccine against the pH1N1 challenge virus was investigated in enzyme-linked immunosorbent assay (ELISA) using plates coated with pH1N1 virion particles expressing native hemagglutinin (HA) spikes. WIV-H1N2 vaccine elicited cross-reactive anti-pH1N1–binding immunoglobulin G (IgG) antibodies comparable to the binding observed with WIV-H1N1–immunized pig sera (Fig. 2E, animals 11 to 20 versus animals 1 to 10).

The functional activity of the immune sera was evaluated in hemagglutination inhibition (HI) assay against the vaccine strain (H1N2) and the challenge strain (pH1N1). Before pH1N1 virus challenge, the

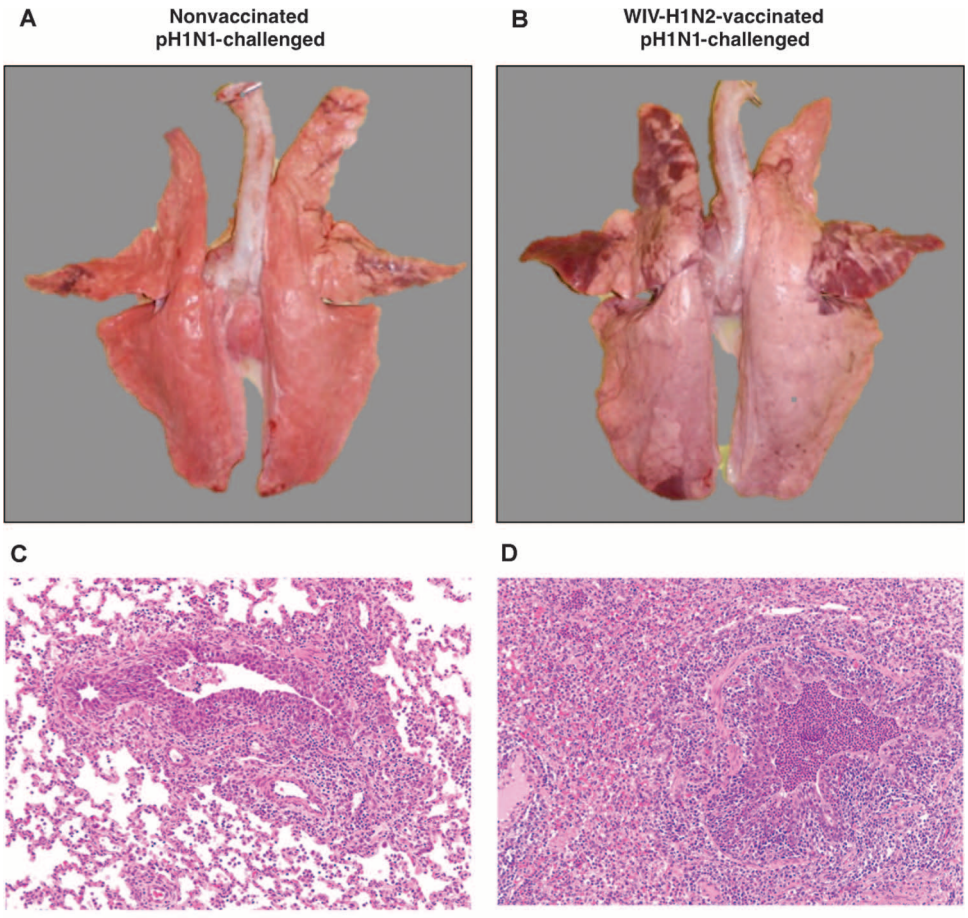

E

LRT lesions	WIV-H1N2-IM	SEM	Sham-IM	SEM
% Macroscopic lesion	18.0	2.0	6.0	1.2
Microscopic lung score (0-21)	16.0	1.0	6.0	1.0

Fig. 1. Heterologous vaccination with WIV-H1N2 led to VAERD in vaccinated pigs after challenge with pH1N1. (**A** to **D**) Representative macroscopic and microscopic lesions in nonvaccinated (n = 10) (A and C) and WIV-H1N2–vaccinated pigs (n = 10) (B and D) 5 days after pH1N1 challenge. Pigs in the WIV-H1N2–vaccinated/pH1N1-challenged group had a greater percentage of lung involvement including macroscopic changes, as well as more severe microscopic lesions (B and D, respectively) compared to the nonvaccinated challenge group (A and C). (C and D) Hematoxylin and eosin–stained histopathological sections, ×200. (**E**) Average percentage macroscopic lung lesions and microscopic lung score for all the animals in each group (10 animals per group). LRT, lower respiratory tract; IM, intramuscular.

WIV-H1N2–vaccinated animals had HI titers against the H1N2 vaccine strain but not against the heterologous pH1N1 virus (Table 1; animals 11 to 20). A positive control group, vaccinated with pH1N1 whole inactivated virus (WIV-H1N1) (Table 1; animals 1 to 10), generated HI titers against pH1N1 but not against the mismatched H1N2 strain. Similar observations of only homologous neutralization were observed in the virus neutralization assay. As expected, all WIV-H1N1–vaccinated pigs were fully protected from pH1N1 challenge (Table 1).

Sequence alignment and phylogenetic relatedness of the H1N2 vaccine and pH1N1 challenge virus HA protein are shown in figs. S1 and S2. The overall amino acid identity in HA between the H1N2 vaccine strain (A/Swine/Minnesota/02011/08) and the pH1N1 challenge strain (A/California/04/2009) was 78%. However, the similarity was disproportionate across the HA, with sequence identity of only 71% in the HA1 domain but a higher sequence homology of 89% in the HA2 domain (*8*).

To understand the disparity between pH1N1 virion–binding antibodies and lack of cross-reactive HI-neutralizing antibodies, we sought to determine whether postvaccination sera from the two vaccine groups contained antibodies that bind differentially to HA1 and HA2 domains of pH1N1. Recombinant HA1 and HA2 proteins of the pH1N1 strain previously demonstrated to be properly folded and to display conformational epitopes were used to coat SPR chips (*9*–*11*). Postvaccination sera from all animals vaccinated with the WIV-H1N1 vaccine (animals 1 to 10 in Table 1) bound strongly to both pH1N1-HA1 and pH1N1-HA2 domains, with higher antibody binding (max RU values) to HA1 than to HA2 (Fig. 2, A versus C). In contrast, the WIV-H1N2 immune sera (from pigs 11 to 20 in Table 1) had no measurable antibody reactivity against the pH1N1-HA1 domain (Fig. 2B). However, the same sera displayed cross-reactive binding antibodies to pH1N1-HA2 with higher titers (maximal RU values) compared with the binding of WIV-H1N1 immune sera to HA2 domain (Fig. 2, C versus D).

Sera from WIV-H1N2–vaccinated pigs enhanced pH1N1 infection of Madin-Darby canine kidney cells

Because WIV-H1N2 elicited antibodies that did not bind to pH1N1-HA1 domain, it was not surprising that they did not neutralize pH1N1 virus in the HI assay (Table 1). To evaluate the influenza infection–modifying potential of these cross-reactive binding antibodies, we performed a Madin-Darby canine kidney (MDCK)–based pH1N1 virus infection assay. Unexpectedly, we observed that all WIV-H1N2 postvaccination sera enhanced pH1N1 infection of MDCK cells in a concentration-dependent manner (Fig. 3A). At the lowest serum dilution (1:20), pH1N1 virus infectivity ranged from 165 to 180% for virus incubated with post-H1N2 vaccination sera compared with virus-only control. No enhancement was observed with any of the prevaccination sera (Fig. 3A, black line). On the other hand, as expected, immune sera from WIV-pH1N1–vaccinated pigs completely inhibited pH1N1 virus infectivity in the MDCK-based assay (Fig. 3, D and E, black curves), in agreement with the HI data (Table 1, animals 1 to 10).

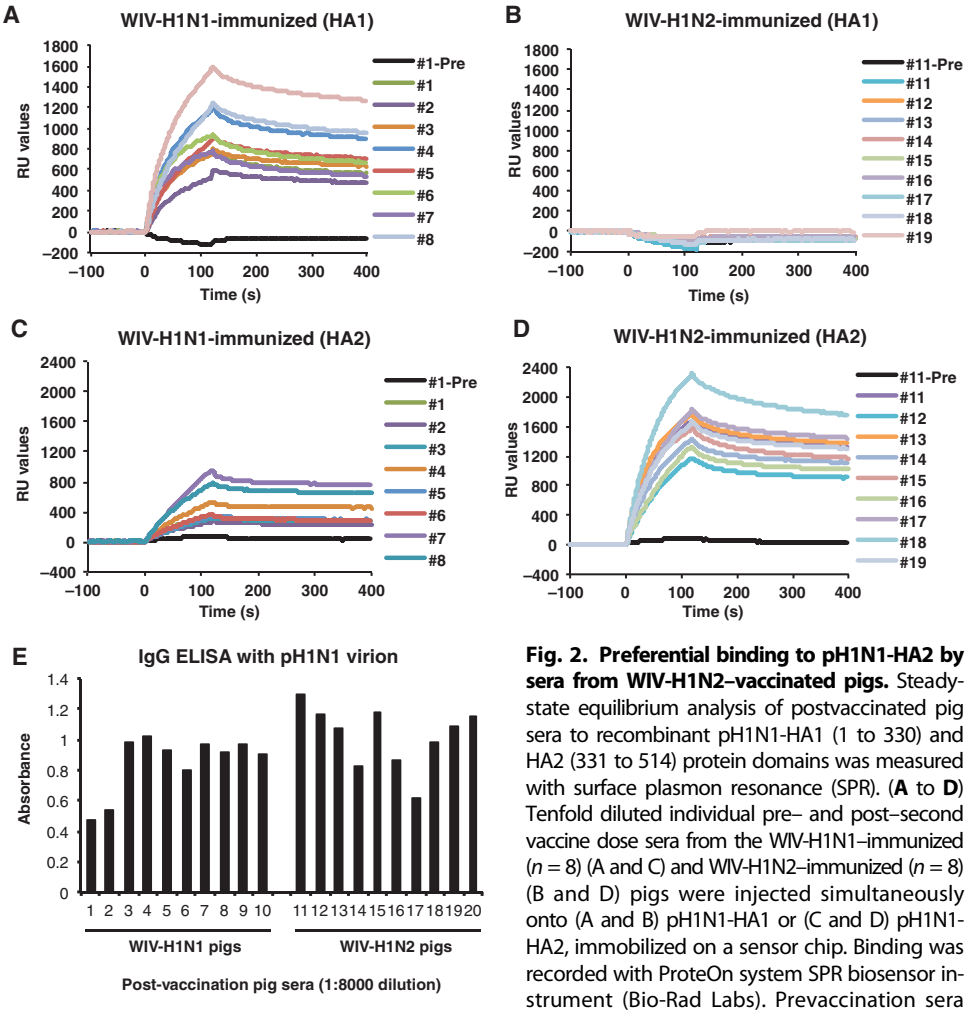

Fig. 2. Preferential binding to pH1N1-HA2 by sera from WIV-H1N2–vaccinated pigs. Steady-state equilibrium analysis of postvaccinated pig sera to recombinant pH1N1-HA1 (1 to 330) and HA2 (331 to 514) protein domains was measured with surface plasmon resonance (SPR). (**A** to **D**) Tenfold diluted individual pre– and post–second vaccine dose sera from the WIV-H1N1–immunized ($n = 8$) (A and C) and WIV-H1N2–immunized ($n = 8$) (B and D) pigs were injected simultaneously onto (A and B) pH1N1-HA1 or (C and D) pH1N1-HA2, immobilized on a sensor chip. Binding was recorded with ProteOn system SPR biosensor instrument (Bio-Rad Labs). Prevaccination sera were used as controls in each assay (all 16 prevaccination sera did not bind to either HA1 or HA2). Binding of the antibodies to immobilized proteins is shown as resonance unit (RU) values. (**E**) Binding of postvaccination pig sera (at 1:8000 dilution) to pH1N1 virions with IgG-based ELISA.

To further explore the specificity of the pH1N1 infection–enhancing antibodies, we adsorbed WIV-H1N2 immune sera with pH1N1-HA2 protein. As can be seen in Fig. 3B, the unbound flow-through serum fractions were devoid of pH1N1 infection–enhancing activity, whereas the HA2-eluted fractions demonstrated enhanced pH1N1 infectivity ranging from 170 to 190% of prevaccination/pH1N1 control cultures at the lowest sera dilution (Fig. 3C). The bound fraction eluted from the HA2 column contained only IgG, and the enhancement could be titered out by serial dilution of the eluted antibodies (Fig. 3C). This suggests that the WIV-H1N2 immune sera contained cross-reactive pH1N1-HA2–targeting antibodies that could increase the infectivity of pH1N1 in MDCK cells.

WIV-H1N2–induced infection-enhancing antibodies compete with pH1N1-neutralizing antibodies in MDCK-based infection assay

In the likely scenario of preexisting anti-HA2 antibodies (from previous seasonal influenza infections or vaccinations) during pH1N1 infection, it was important to determine whether the infection-enhancing anti-HA2 antibodies could diminish the effectiveness of pH1N1-HA1–targeting neutralizing antibodies. We mimicked this scenario by serially diluting immune serum from WIV-H1N1–vaccinated pig in the presence of HA2-eluted antibodies from WIV-H1N2 immune serum (at 1:500 dilution of initial sera concentration) (Fig. 3, D and E, and fig. S3). The pH1N1-specific immune serum demonstrated a typical neutralization curve that was not changed in the presence of prevaccination serum from the WIV-H1N2–vaccinated pigs (Fig. 3, D and E, black versus broken red curves). However, in the presence of WIV-H1N2 HA2-eluted antibodies (1:500), pH1N1 virus neutralization was reduced even at the lowest WIV-H1N1 serum dilution (that is, only 20% neutralization at a 1:100 WIV-H1N1 serum dilution). At higher dilutions of WIV-H1N1 immune serum (>1:400), a modest enhancement of virus infection was observed in the presence of WIV-H1N2 HA2-eluted antibodies (Fig. 3, D and E, and fig. S3). Thus, although the WIV-H1N2–induced pH1N1 infection–enhancing antibodies are only cross-reactive to the pH1N1-HA2 domain, they can compete and/or compromise the neutralizing activity of pH1N1-neutralizing antibodies that target primarily the HA1 globular head, especially when HA1-specific, neutralizing antibodies were present at low titers.

Elucidation of post-H1N2 vaccination serum antibody epitope repertoire using pH1N1 genome-fragment phage display library identified an immunodominant epitope close to HA2 fusion peptide

We previously used genome-fragment phage display library (GFPDL) displaying peptide sequences of pH1N1 HA to probe the epitope diversity of polyclonal postvaccination and post-infection human sera (*10*–*12*). Here, we compared the epitope profiles of polyclonal serum antibodies generated by vaccination with WIV-H1N1 or WIV-H1N2 in pigs. No phages bound to the prevaccination pig sera in either of the vaccine groups (Fig. 4A). The WIV-H1N1 immune sera contained antibodies that selected phage-displayed peptides mapping primarily to pH1N1-HA1, including the receptor-binding domain (RBD) (Fig. 4A, red and yellow bars), and to a lesser extent to HA2 (blue bars), in agreement with the data in SPR (Fig. 2, A and C). In contrast, WIV-H1N2 immune sera bound to a predominant minimal epitope in pH1N1-HA2 (amino acids 32 to 77 in the pH1N1-HA2 sequence; shown in bold red letters), downstream of the fusion peptide (amino acids 1 to 25; shown in bold black letters) (Fig. 4, A and B). WIV-H1N2 antibodies also bound a short peptide mapping to the N terminus of HA1 (amino acids 1 to 48), but all binding antibodies were of IgM isotype, as determined by SPR (fig. S4), which are expected to be of low avidity.

Table 1. WIV-H1N2 does not generate pH1N1-neutralizing antibodies.

Vaccine	Pig no.	HI titer to H1N2*		HI titer to pH1N1*		pH1N1 challenge outcome
		Prevaccination	Postvaccination	Prevaccination	Postvaccination	
WIV-H1N1 (2×)	1	<10	<10	<10	160	Protection
	2	<10	<10	<10	320	Protection
	3	<10	<10	<10	80	Protection
	4	<10	<10	<10	320	Protection
	5	<10	<10	<10	160	Protection
	6	<10	<10	<10	160	Protection
	7	<10	<10	<10	80	Protection
	8	<10	<10	<10	80	Protection
	9	<10	<10	<10	160	Protection
	10	<10	<10	<10	160	Protection
WIV-H1N2 (2×)	11	<10	80	<10	<10	VAERD
	12	<10	80	<10	<10	VAERD
	13	<10	80	<10	<10	VAERD
	14	<10	160	<10	<10	VAERD
	15	<10	80	<10	<10	VAERD
	16	<10	40	<10	<10	VAERD
	17	<10	80	<10	<10	VAERD
	18	<10	160	<10	<10	VAERD
	19	<10	80	<10	<10	VAERD
	20	<10	80	<10	<10	VAERD

*Endpoint titers (mean of three replicates) with polyclonal swine sera in an HI assay.

The location of the predominant HA2 epitope bound by the WIV-H1N2 sera is shown on the structure of the pH1N1 HA trimer in relation to the fusion peptide (Fig. 4C, red and black segments, respectively). The identified immunodominant HA2 epitope (shown in red) is surface-exposed and should be available for binding to antibodies on the trimeric HA spikes on the intact influenza virions.

Anti-HA2 antibodies in WIV-H1N2–immunized pig sera enhanced pH1N1-mediated virus membrane fusion

Influenza virus entry into cells proceeds through multiple stages. The influenza HA binds to sialic acid receptors on the surface of host cells, leading to rapid internalization into endosomes. Upon internalization, the virus is exposed to lower pH values that trigger conformational changes in HA, resulting in virus–cell membrane fusion (*13*). New antiviral drugs designed to prevent acid-dependent virus membrane fusion are under evaluation (*14*).

Therefore, the enhanced pH1N1 virus infection in the MDCK assay in the presence of anti–WIV-H1N2 antibodies could be mediated by either increased virus receptor binding or enhanced fusion of virus after acidic pH–induced HA conformational changes in the endosomes. To investigate the impact of anti-HA2 antibodies on pH1N1 virus–sialic acid receptor binding, we quantified direct binding of pH1N1 virions to sialic acid glycoprotein (fetuin) in SPR, and in the red blood cell (RBC) hemagglutination assay in the absence and presence of pre- and postvaccination pig sera. WIV-H1N2 postvaccination sera did not significantly influence pH1N1 virus receptor-binding activity in either assay (figs. S5 and S6). Moreover, because MDCK cells do not express Fc receptors (*15*), it was unlikely that Fc-mediated endocytosis played a role in the observed enhanced pH1N1 virus infection.

Hemolysis assay is widely used as a functional biological assay to study influenza virus–mediated fusion activity (*16*, *17*). Because the HA2-targeting antibodies in the postvaccination sera mapped to a site very close to the fusion peptide (Fig. 4), we examined their effect on pH1N1 virus fusion using the RBC hemolysis assay. To that end, pH1N1 virus was incubated with sera at room temperature, then mixed with fresh human erythrocytes (2% suspension), and incubated at 4°C. To trigger fusion of viral and cellular membrane, we added sodium citrate (pH 5.2) and continued incubation at 37°C for 90 min, resulting in HA acidification. This leads to conformational changes that trigger fusion, resulting in RBC hemolysis. The amount of heme released from RBC in the supernatant is directly proportional to virus–cell membrane fusion.

All WIV-H1N2 postvaccination sera from individual animals enhanced pH1N1-mediated virus–cell membrane fusion by 250 to 300% compared with virus only (no antibody) or pH1N1 virus mixed with prevaccination sera (Fig. 5A, red versus black and blue bars). In contrast, WIV-H1N1 immune sera containing neutralizing antibodies prevented the acid-induced RBC hemolysis by blocking virus binding/entry (Fig. 5A, three right columns). To confirm the specificity of the fusion-enhancing antibodies, we subjected individual WIV-H1N2 postvaccination sera over a pH1N1-HA2 column and compared the activity of unbound flow-

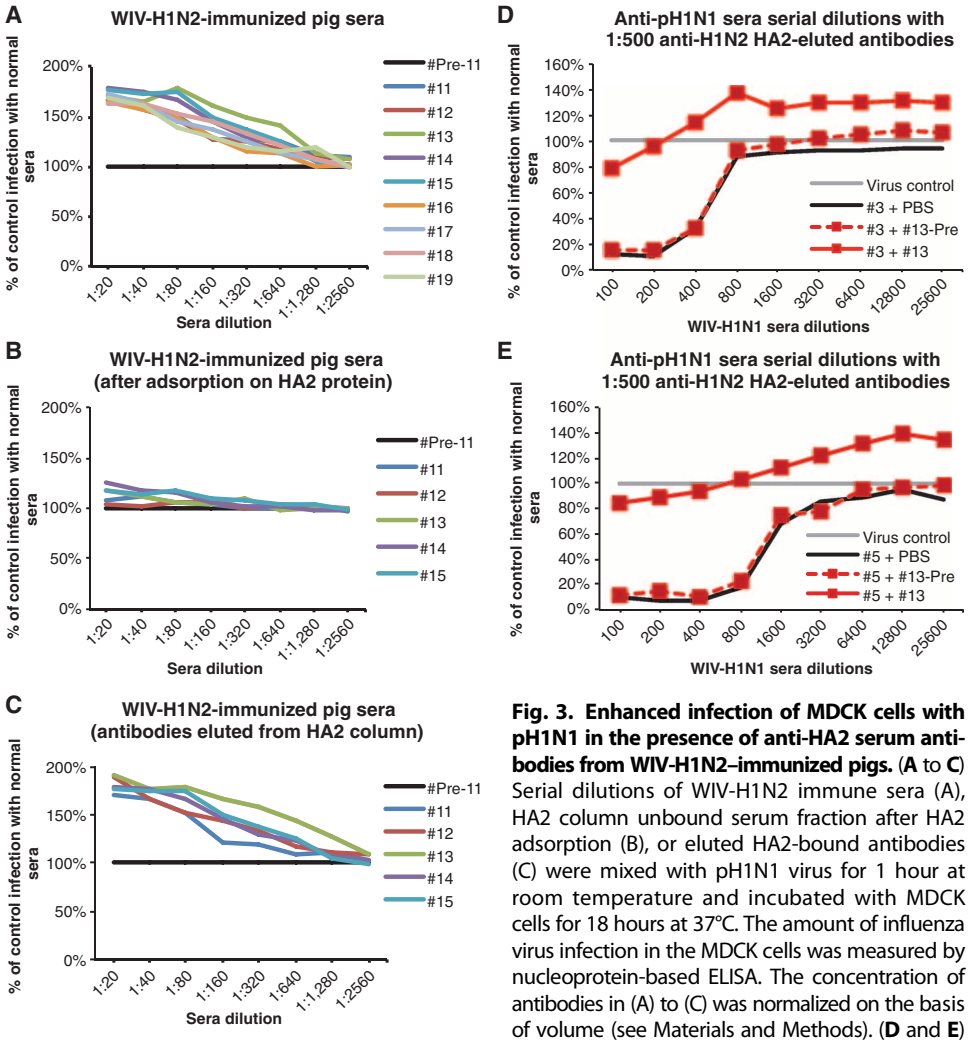

Fig. 3. Enhanced infection of MDCK cells with pH1N1 in the presence of anti-HA2 serum antibodies from WIV-H1N2–immunized pigs. (**A** to **C**) Serial dilutions of WIV-H1N2 immune sera (A), HA2 column unbound serum fraction after HA2 adsorption (B), or eluted HA2-bound antibodies (C) were mixed with pH1N1 virus for 1 hour at room temperature and incubated with MDCK cells for 18 hours at 37°C. The amount of influenza virus infection in the MDCK cells was measured by nucleoprotein-based ELISA. The concentration of antibodies in (A) to (C) was normalized on the basis of volume (see Materials and Methods). (**D** and **E**) Anti-HA2 antibodies can compete with pH1N1-neutralizing antibodies. Serial dilutions of different WIV-pH1N1–immunized pig sera (D and E) were mixed with prevaccination sera or post–WIV-H1N2 HA2-eluted antibodies (diluted 1:500), incubated with pH1N1 virus, and used for MDCK infection as in (A) to (C). The virus titer as determined by nucleoprotein-based ELISA is expressed as "% of control infection" as given by the following formula: ([A_{490} (experimental) − A_{490} (no virus added)]/[A_{490} (pH1N1 virus control with prevaccination sera) − A_{490} (no virus added)] × 100%). Similar data generated with HA2-binding antibodies from additional pigs in WIV-H1N2 vaccine groups are presented in fig. S3.

through (HA2-depleted) versus bound-eluted (HA2-enriched) antibodies (Fig. 5B, blue versus red bars). These data strongly suggest that the anti–pH1N1-HA2 cross-reactive antibodies in the WIV-H1N2 immune sera increased pH1N1 virus infection of MDCK cells by enhancing pH1N1 virus fusion.

To further investigate the correlation between the observed pH1N1 virus fusion–enhancing activity in the sera of WIV-H1N2–vaccinated pigs and VAERD observed in individual pigs, we plotted the percentage of macroscopic lung lesions of WIV-H1N2–vaccinated and pH1N1-challenged animals (11 to 19) with the levels of fusion-enhancing antibody activity in the corresponding pig sera. As can be seen in Fig. 5C, a significant positive correlation was observed between the percentage of RBC hemolysis and the percentage of macroscopic lung lesions of individual WIV-H1N2–immunized pigs (R^2 = 0.68; P = 0.0000044).

These findings suggest a possible direct role for virus fusion–promoting activity of cross-reactive HA2-targeting antibodies induced by heterologous vaccination in the observed enhanced lung pathology in animals associated with VAERD after mismatched influenza virus challenge.

DISCUSSION

Our study was set up to explore the VAERD observed in pH1N1-challenged pigs after heterologous (mismatched) vaccination with human-like WIV-H1N2 vaccine (*6*, *7*).

The main findings in this study were as follows. (i) No cross-reactive pH1N1-specific HI titers or virus neutralization titers were observed after vaccination of pigs with heterologous WIV-H1N2 vaccine. Unexpectedly, post–WIV-H1N2 vaccination sera enhanced infection of MDCK cells with pH1N1. (ii) WIV-H1N2 vaccination elicited pH1N1-HA cross-reactive antibodies that bound exclusively to the pH1N1-HA2 stalk and mapped to an epitope immediately downstream of the fusion peptide (amino acids 32 to 77) of HA2. (iii) The WIV-H1N2–induced pH1N1 cross-reactive antibodies that were eluted from HA2 column mediated the MDCK-enhanced infection. (iv) These HA2-specific antibodies did not change pH1N1 virus receptor binding but demonstrated pH1N1 virus–mediated fusion-enhancing activity in a pH-dependent influenza virus RBC hemolysis assay. (v) Strong correlation between lung pathology and the corresponding levels of fusion-enhancing antibody activity was observed for individual VAERD-affected pigs in the WIV-H1N2–primed pH1N1 virus–challenged group.

Therefore, because of low antigenic conservation of the HA1 globular domain, vaccination with whole inactivated influenza virus vaccine resulted in the absence of cross-reactive neutralizing antibodies against the mismatched influenza virus challenge strain, similar to the scenario of antigenic shift of influenza viruses. However, induction of high-titer cross-reactive antibodies against the more conserved HA2 stalk domain may result in virus fusion enhancement that could contribute to more severe in vivo lung pathology after infection with the heterologous strain of influenza virus. We also found that immune sera from WIV-pH1N1–vaccinated pigs, containing pH1N1-neutralizing antibodies, ameliorated the enhanced pH1N1-MDCK cell infection mediated by WIV-H1N2–induced anti-HA2 antibodies, but this effect was diminished by dilution of the pH1N1-neutralizing antibodies. Therefore, our study revealed a delicate

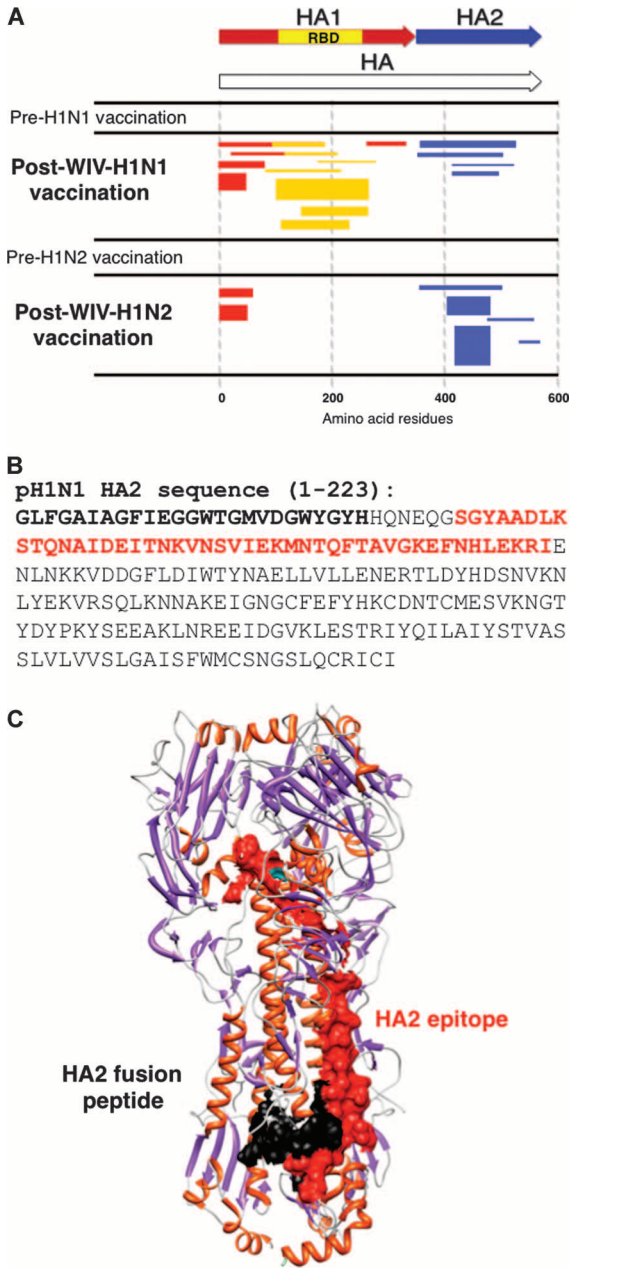

Fig. 4. Elucidation of antibody repertoires elicited after vaccination of pigs with inactivated WIV-H1N1 or WIV-H1N2 vaccine. (**A**) Schematic alignment of the peptides from phage clones after affinity selection with GFPDL-expressing HA peptides of pH1N1 influenza A/California/04/2009 on sera obtained from prevaccination sera and WIV-H1N1– or WIV-H1N2–vaccinated pigs. To determine the diversity of the epitopes, we sequenced all of the eluted phage clones after panning, and we aligned peptide sequences displayed on the selected phage clones to the pH1N1 influenza HA. Color code of bars representing phage-displaying peptides: red, HA1; yellow, RBD; blue, HA2. The horizontal position and the length of the bars indicate the peptide sequence displayed on the selected phage clone aligned with the influenza HA. The thickness of each bar represents the frequencies of repetitively isolated phage inserts. The numbers on the *x* axis depict the amino acid residues for the corresponding pH1N1-HA used for alignment. (**B**) The immunodominant minimal HA2 epitope in the pH1N1 HA recognized by WIV-H1N2 pig sera is depicted in bold red within the pH1N1-HA2 sequence, whereas the fusion peptide sequence is shown in the bold black. (**C**) Immunodominant cross-reactive HA2 epitope recognized by WIV-H1N2 immune sera is shown as surface-exposed colored patches (red) on one HA monomer within the HA trimer structure [Protein Data Bank (PDB) identifier 3LZG]. The fusion peptide is depicted in black. These regions are shown in the side view.

balance between neutralizing antibodies targeting primarily the RBD in HA1 and nonneutralizing fusion-enhancing HA2 cross-reactive antibodies, which is likely to determine the clinical outcome of mismatched influenza virus infection, especially if the neutralizing antibodies have not reached a critical threshold during early time points after infection.

One of the limitations of the current study is that it was conducted in pig model with a particular combination of mismatched vaccine and challenge influenza virus strains, and extrapolation to human influenza vaccination scenarios may not be obvious. However, the pig model was shown to be an exceptionally good model for human influenza and vaccine studies. Pigs are a natural influenza host, express similar receptor types as humans in a similar distribution (*18*–*21*), and are infected with the same influenza subtypes as humans (*21*–*23*). They are connected with humans in the overall ecology of influenza, trading viruses back and forth (*22*), and display similar influenza-induced clinical illness. Additionally, pigs and humans have similar genetics, anatomy and physiology, and immune systems, much more so than laboratory animal models (*24*–*26*). Similar to humans, pigs are routinely vaccinated against the circulating influenza strains with multicomponent vaccines. The H1 δ-cluster of endemic swine influenza viruses represented by the H1N2 virus is a spillover from human seasonal H1N1 and is now a future risk to humans as it evolves in pigs. The pH1N1 HA is from the swine classical H1N1 lineage. Furthermore, the VAERD phenomenon observed in pigs can be reproduced in multiple mismatched vaccination heterologous influenza virus challenge studies, either by vaccinating with WIV-H1N2 and challenging with pH1N1 (in the current study) or by vaccinating with pH1N1 vaccine followed by challenge with H1N2 (*27*).

Another possible limitation of the study is the use of young piglets (<6 months) with limited or no preexisting anti-influenza antibodies. This model mimics young infants, and the outcome of heterologous vaccination followed by mismatched challenge influenza strain may differ in adults, depending on the levels of preexisting HA1- and HA2-specific B cells and the affinity of their B cell receptors. However, the current study may also be relevant to the population as a whole (or high-risk subsets) when a markedly shifted influenza virus emerges and causes a pandemic.

Recently, broadly neutralizing antibodies have been identified that bind conserved epitopes in the HA2 stem region. These antibodies are reported to neutralize the influenza virus by preventing the pH-dependent HA conformational changes, leading to fusion of viral and cellular membranes (*28*–*32*). We mapped the HA2-targeting fusion-enhancing antibodies elicited by WIV-H1N2 vaccine to a region of the pH1N1-HA2 close to the fusion peptide and overlapping epitopes of several stem-targeting broadly neutralizing monoclonal antibodies (mAbs). Our study suggests that vaccine-induced HA2-targeting antibodies may contain competing antibodies with fusion-blocking and fusion-enhancing activities. The titers and affinity of the various antibodies will affect virus fusion in the endosomal compartment (that is, post-binding/internalization) and determine the outcome of the influenza virus infection.

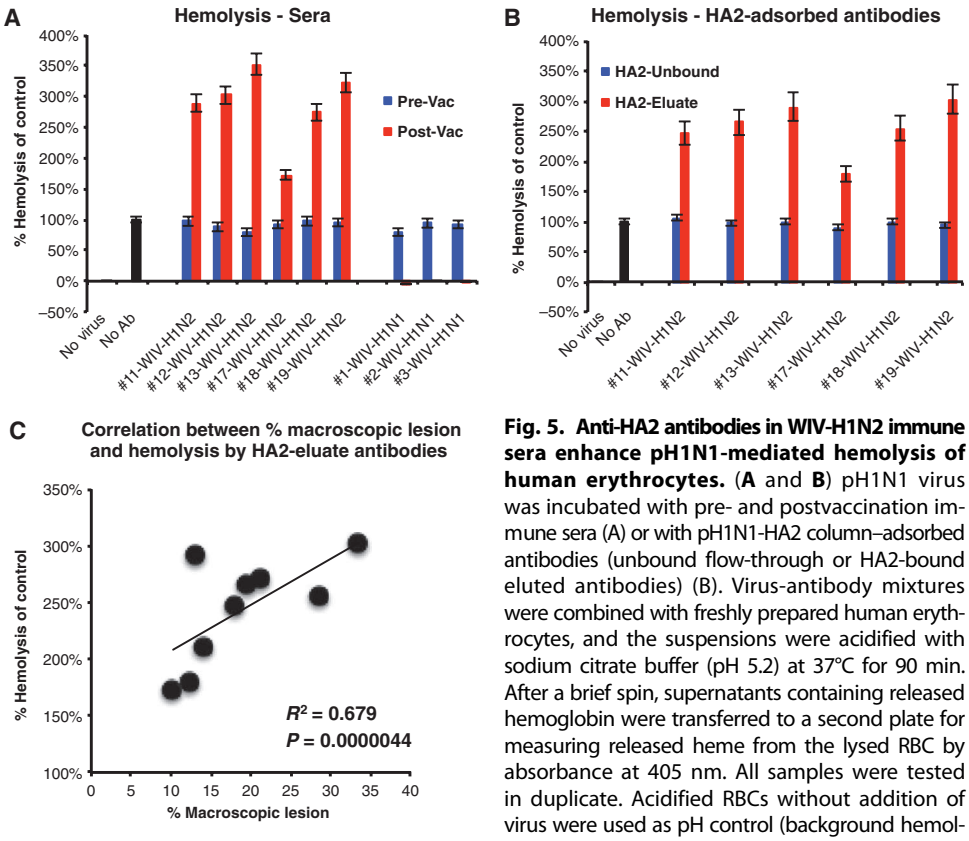

Fig. 5. Anti-HA2 antibodies in WIV-H1N2 immune sera enhance pH1N1-mediated hemolysis of human erythrocytes. (**A** and **B**) pH1N1 virus was incubated with pre- and postvaccination immune sera (A) or with pH1N1-HA2 column–adsorbed antibodies (unbound flow-through or HA2-bound eluted antibodies) (B). Virus-antibody mixtures were combined with freshly prepared human erythrocytes, and the suspensions were acidified with sodium citrate buffer (pH 5.2) at 37°C for 90 min. After a brief spin, supernatants containing released hemoglobin were transferred to a second plate for measuring released heme from the lysed RBC by absorbance at 405 nm. All samples were tested in duplicate. Acidified RBCs without addition of virus were used as pH control (background hemolysis). Virus control (No Ab) for the absorbance observed with pH1N1-RBC mixture in the absence of antibodies was set at 100%. The hemolysis titer is expressed as "% hemolysis of control" as given by the following formula: ([A_{405} (experimental) − A_{405} (no virus added)]/[A_{405} (pH1N1 virus only without antibody) − A_{405} (no virus added)] × 100%). Data are representative of three experiments. (**C**) Positive correlation between hemolytic activity of pH1N1 in the presence of eluted anti-HA2 antibodies from WIV-H1N2 postvaccination sera and macroscopic lung lesions in the WIV-H1N2–immunized pigs (n = 8) after pH1N1 virus challenge was calculated with Spearman correlation coefficient that was statistically significantly calculated with Student's t test for paired samples.

We previously demonstrated that most humans without H5 exposure have cross-reacting nonneutralizing anti-H5N1 antibodies that target HA2, reflecting the high degree of conservation of the HA2 sequence between highly pathogenic H5N1 and seasonal H1N1 virus strains (*33*, *34*). Therefore, introduction of new influenza strains into naïve populations (similar to the 2009 pH1N1 virus) could recall memory B cells to predominantly HA2 cross-reactive epitopes induced by previous vaccination and/or exposure to seasonal influenza strains. Most of such antibodies are expected to be nonneutralizing and potentially capable of enhancing virus fusion. In the presence of below-threshold titers of anti-HA1 antibodies, it is possible that nonneutralized HA2 antibody–bound virions can enter the endosomal compartment and undergo the conformational changes that promote virus fusion and enhance virus infection.

During the 2009 H1N1 influenza pandemic (pH1N1), severe disease in pH1N1-infected individuals was associated with low-avidity antibodies forming immune complexes (complement binding) in several patient's lungs (*35*). More recently, To *et al.* found that patients with severe disease (requiring ventilation) had significantly higher ratios of ELISA-binding titers/virus-neutralizing titers compared with less severe cases. This study concluded that high titers of nonneutralizing antibodies with higher avidity at the early stage of influenza virus infection may be associated with worse clinical severity and poorer outcome (*36*). However, in both the Monsalvo and To studies, the specificity of the antibodies was not established.

Our data do not exclude other mechanisms of VAERD, including T helper 1 (T_H1)/T_H2/T regulatory (T_{reg}) imbalance, high proinflammatory cytokines, and infiltration of neutrophils (*7*, *37*–*40*). However, the lack of high-avidity neutralizing antibodies that prevent virus attachment to its cellular receptors seems to be an important component of most reported VAERD (*2*, *41*–*44*). Our findings suggest that the specificity and activity of nonneutralizing antibodies should be further evaluated in cases of VAERD.

In conclusion, we have identified cross-reacting pH1N1-HA2–binding antibodies induced by heterologous inactivated influenza A vaccination that targets an immunodominant epitope close to the fusion peptide, leading to enhanced pH1N1 virus fusion. Such antibodies were correlated with VAERD after heterologous pH1N1 influenza virus challenge. These findings propose a new mechanism of influenza VAERD that should be monitored during human vaccinations in the face of emerging influenza strains with low antigenic cross-reactivity with seasonal influenza strains. Such antibodies should also be evaluated in the immune response during development of universal influenza vaccines designed to primarily target the influenza virus HA2 stem region with the exclusion of the HA1 globular head.

MATERIALS AND METHODS

Pig vaccination, challenge, and pathologic examination of lungs

Three-week-old cross-bred pigs were obtained from a herd free of influenza A virus and porcine reproductive and respiratory syndrome virus and treated with ceftiofur crystalline free acid (Pfizer Animal Health) and enrofloxacin injectable solution (Bayer Animal Health) according to label directions to reduce bacterial contaminants before the start of the study. Pigs were randomly assigned to treatment groups and housed in biosafety level 2 and cared for in compliance with the Institutional Animal Care and Use Committee of the National Animal Disease Center.

WIVs were prepared with about 128 HA units of virus, inactivated by ultraviolet irradiation, and adjuvanted with a commercial oil-in-water emulsion (MVP Technologies), and the experimental design was conducted as previously described (*6*). Pigs were vaccinated intramuscularly

at about 4 weeks of age and boosted at 7 weeks of age. Postboost serum was collected at about 10 weeks of age, just before challenge.

Ten vaccinated pigs per group and 10 nonvaccinated pigs were challenged at about 10 weeks of age by intratracheal route with 2 ml of 1×10^5 median tissue culture infectious dose ($TCID_{50}$)/ml of pH1N1 (A/California/04/2009) propagated in MDCK cells. At necropsy, lungs were removed and evaluated for the percentage of the lung affected with purple-red consolidation typical of influenza A virus in swine. The percentage of the surface area affected with pneumonia was visually estimated for each lung lobe, and the total percentage for the entire lung was calculated on the basis of weighted proportions of each lobe to the total lung volume (*7*, *45*). Tissue samples from the trachea and right middle or affected lung lobe were fixed in 10% buffered formalin for histopathologic examination. Tissues were processed by routine histopathological procedures, and slides were stained with hematoxylin and eosin. Microscopic lesions were evaluated by a veterinary pathologist blinded to treatment groups. Individual scores were assigned to each of six parameters to adequately reflect the contribution of each lesion associated with VAERD: bronchial and bronchiolar epithelial necrosis or proliferation, suppurative bronchitis or bronchiolitis, peribronchiolar lymphocytic cuffing, and alveolar septal thickening with inflammatory cells (interstitial pneumonia). The first two scores focused on the intrapulmonary airways typical of influenza A infection: (i) percentage of bronchi and bronchioles affected with epithelial lesions (necrotizing or proliferative bronchitis and bronchiolitis) (0 to 4), and (ii) percentage of bronchi and bronchioles that contained purulent exudate (suppurative bronchitis or bronchiolitis) (0 to 4). Four additional lung lesion scores associated with VAERD were based on the following: (iii) magnitude of peribronchiolar lymphocytic cuffing (0 to 3), (iv) presence and severity of alveolar septal inflammation (interstitial pneumonia) (0 to 4), (v) presence and severity of alveolar and interlobular edema (0 to 3), and (vi) presence and magnitude of epithelial exocytosis (intraepithelial microabscesses) (0 to 3). A composite score was computed with the sum of the six individual scores (0 to 21).

Hemagglutination inhibition

HI assays were conducted with A/Swine/Minnesota/02011/08 (H1N2) or A/California/04/2009 (pH1N1) virus as antigen and turkey RBCs as indicators with standard techniques (World Health Organization manual). Reciprocal titers were divided by 10 and $\log_2$-transformed, analyzed, and reported as the geometric mean.

Sequence analysis

The evolutionary history of HA amino acid sequences was inferred with the neighbor-joining method in MEGA5 (*46*). The tree was drawn to scale, with branch lengths in the same units as those of the evolutionary distances used to infer the phylogenetic tree. Evolutionary distances were computed with the Poisson correction method in the units of the number of amino acid substitutions per site. The analysis involved 66 amino acid sequences. All ambiguous positions were removed for each sequence pair. There were a total of 570 positions in the final data set. Pairwise comparison of the amino acid sequences of A/California/04/2009 and A/Swine/Minnesota/02011/08 HA sequences was conducted with ClustalW.

Binding of postvaccination sera to pH1N1 virions in ELISA

ELISA to detect total IgG antibodies present in serum against whole-virus preparations of pH1N1 was performed as previously described (*5*) with modifications. Concentrated virus was resuspended in tris-EDTA basic buffer (pH 7.8) and diluted to an HA concentration of 100 HA units/50 μl. Immulon 2 HB 96-well plates (Dynex) were coated with 100 μl of antigen solution and incubated at room temperature overnight. Sera were diluted 1:8000 in phosphate-buffered saline (PBS), and the assays were performed on each sample in duplicate. The mean optical density of duplicate wells was calculated.

MDCK cell–based virus infection assay

pH1N1 virus–neutralizing/enhancing activity in vaccinated pig sera was analyzed for days 0 and 56 (before primary vaccination and after second vaccination, respectively) in a virus infection assay on the basis of the method used in the pandemic influenza reference laboratories of the Centers for Disease Control and Prevention (*9*) with low-pathogenicity reassortant pH1N1 virus generated by reverse genetics (X-179A). The experiments were conducted with three replicates for each serum sample and performed at least twice. The virus titer as determined by nucleoprotein-based ELISA is expressed as % of control infection with normal sera as given by the following formula: $([A_{490}$ (experimental) $- A_{490}$ (no virus added)$]/[A_{490}$ (pH1N1 virus with prevaccination sera) $- A_{490}$ (no virus added)$] \times 100\%)$. Prevaccination sera were used as control and had no effect on virus infection.

Epitope mapping of postvaccination polyclonal pig sera by panning with pH1N1 GFPDLs

The H1N1pdm09 phage display library affinity selection performed in the current study was done as previously described (*10*). For GFPDL panning with postvaccination pig sera, equal volumes of sera collected after two vaccine doses from three pigs of each vaccine group (WIV-H1N1 or WIV-H1N2) were pooled.

Binding kinetics of polyclonal serum antibodies pH1N1-HA1 and pH1N1-HA2 protein domains by SPR

Steady-state equilibrium binding of postvaccination individual pig sera was monitored at 25°C with a ProteOn SPR biosensor (Bio-Rad) as previously described (*10*). The pH1N1-rHA proteins were coupled to a GLC sensor chip with amine coupling with 500 RU in the test flow cells. Samples of 60 μl of freshly prepared sera at 10-fold dilutions were injected at a flow rate of 30 μl/min (120-s contact time) for association, and dissociation was performed over a 600-s interval (at a flow rate of 30 μl/min). Responses from the protein surface were corrected for the response from a mock surface and for responses from a separate, buffer-only injection. mAb 2D7 (anti-CCR5) was used as a negative control in these experiments. Total antibody binding was determined directly from the serum sample interaction with rHA1 (1 to 330) and rHA2 (331 to 514) protein domains of the pH1N1 virus by SPR with the Bio-Rad ProteOn manager software as described before (*11*). The antigen-antibody measurements were determined from two independent SPR runs.

Receptor-binding assay with SPR

Binding of pH1N1 virus in the absence or presence of serum antibodies to fetuin (natural homolog of sialic acid cell surface receptor proteins) and its asialyted counterpart (asialofetuin) was analyzed at 25°C with a ProteOn SPR biosensor (Bio-Rad Labs). Fetuin or asialofetuin (Sigma) was coupled to a GLC sensor chip with amine coupling at 1000 RU in the test flow cells. Samples of 60 μl of freshly prepared pH1N1 virus in the absence or presence of serum antibodies were

injected at a flow rate of 30 μl/min (120-s contact time). The flow was directed over a mock surface to which no protein was bound, followed by the fetuin- or asialofetuin-coupled surface. Responses from the protein surface were corrected for the response from the mock surface and for responses from a separate, buffer-only injection. Binding kinetics and data analysis were performed with Bio-Rad ProteOn manager software (version 2.0.1).

Influenza virus–induced hemolysis assay

Hemolysis titrations were performed in 96-well round-bottom polystyrene microtiter plates. pH1N1 virus concentrate containing 200 HA units (25 μl) was incubated with serial twofold dilution of antibodies (25 μl) for 30 min at room temperature. Fresh human erythrocytes were washed thrice with 0.15 M NaCl and resuspended to make a 2% (v/v) suspension in 0.15 M NaCl. After incubating virus-antibody mixture at room temperature for 30 min, 50 μl of 2% human erythrocytes was added to the virus-antibody mixture and incubated at 4°C for another 20 min. To trigger hemolysis, we added 200 μl of sodium citrate (0.15 M) at pH 5.2 and mixed it well with erythrocyte suspension. The mixture was incubated at 37°C for 90 min for HA acidification and hemolysis. To separate nonlysed erythrocytes, we centrifuged the plates at the end of incubation at 800*g* for 5 min. The supernatant (100 μl) was transferred to another flat-bottom 96-well plate. The heme of lysed RBCs that was released into the supernatant was quantified by measuring its absorbance at 405 nm with a BioTek plate reader.

The hemolysis titer is expressed as % hemolysis of control as given by the following formula: $([A_{405}$ (experimental) $- A_{405}$ (no virus added)]/$[A_{405}$ (pH1N1 virus only) $- A_{405}$ (no virus added)] $\times$ 100%).

Adsorption of serum antibodies with HA proteins

Fivefold diluted post-H1N1 vaccination pig sera (100 μl) were added to 0.5 mg of purified HA2-His_6 protein and incubated for 1 hour at room temperature. Nickel–nitrilotriacetic acid (Ni-NTA) magnetic beads (100 μl) (Qiagen) were added for 20 min at room temperature with end-to-end shaking to capture the His-tagged proteins and the antibodies bound to them, followed by magnetic separation. Supernatants containing the unbound antibodies were collected. The magnetic beads were washed five times with PBS, and HA2-bound antibodies were eluted by incubating beads with 200 μl of 0.1 N HCl (adjusted to pH 2.2 with glycine and bovine serum albumin) for 10 min at room temperature on end-to-end shaker. The eluates (184 μl) were collected and neutralized by adding 16 μl of 2 M tris solution. The pre- and post-adsorbed sera were subjected to MDCK-based pH1N1 virus infection assay.

Statistical analyses

Differences between groups were examined for statistical significance with Student's *t* test. An unadjusted *P* value less than 0.05 was considered to be significant.

SUPPLEMENTARY MATERIALS

www.sciencetranslationalmedicine.org/cgi/content/full/5/200/200ra114/DC1

Fig. S1. Pairwise alignment of the HA amino acid sequence of pH1N1 (A/California/04/2009) and H1N2 (A/Swine/Minnesota/02011/2008).

Fig. S2. Phylogenetic tree of HA proteins from human and swine H1 viruses.

Fig. S3. Anti-HA2 antibodies can compete with pH1N1-neutralizing antibodies.

Fig. S4. WIV-H1N2 postvaccination serum antibody binding to N-terminal HA1 domain is mediated by IgM isotype antibody.

Fig. S5. Binding of pH1N1 virus to sialic acid receptor in the absence and presence of WIV-H1N2 sera in SPR assay.

Fig. S6. No enhancement of pH1N1 virus–mediated hemagglutination in the presence of WIV-H1N2 serum antibodies.

REFERENCES AND NOTES

1. H. W. Kim, J. A. Bellanti, J. O. Arrobio, J. Mills, C. D. Brandt, R. M. Chanock, R. H. Parrott, Respiratory syncytial virus neutralizing activity in nasal secretions following natural infection. *Proc. Soc. Exp. Biol. Med.* **131**, 658–661 (1969).
2. F. P. Polack, M. N. Teng, P. L. Collins, G. A. Prince, M. Exner, H. Regele, D. D. Lirman, R. Rabold, S. J. Hoffman, C. L. Karp, S. R. Kleeberger, M. Wills-Karp, R. A. Karron, A role for immune complexes in enhanced respiratory syncytial virus disease. *J. Exp. Med.* **196**, 859–865 (2002).
3. V. A. Fulginiti, J. J. Eller, A. W. Downie, C. H. Kempe, Altered reactivity to measles virus. Atypical measles in children previously immunized with inactivated measles virus vaccines. *JAMA* **202**, 1075–1080 (1967).
4. A. L. Vincent, S. L. Swenson, K. M. Lager, P. C. Gauger, C. Loiacono, Y. Zhang, Characterization of an influenza A virus isolated from pigs during an outbreak of respiratory disease in swine and people during a county fair in the United States. *Vet. Microbiol.* **137**, 51–59 (2009).
5. A. L. Vincent, K. M. Lager, B. H. Janke, M. R. Gramer, J. A. Richt, Failure of protection and enhanced pneumonia with a US H1N2 swine influenza virus in pigs vaccinated with an inactivated classical swine H1N1 vaccine. *Vet. Microbiol.* **126**, 310–323 (2008).
6. P. C. Gauger, A. L. Vincent, C. L. Loving, K. M. Lager, B. H. Janke, M. E. Kehrli Jr., J. A. Roth, Enhanced pneumonia and disease in pigs vaccinated with an inactivated human-like (δ-cluster) H1N2 vaccine and challenged with pandemic 2009 H1N1 influenza virus. *Vaccine* **29**, 2712–2719 (2011).
7. P. C. Gauger, A. L. Vincent, C. L. Loving, J. N. Henningson, K. M. Lager, B. H. Janke, M. E. Kehrli Jr., J. A. Roth, Kinetics of lung lesion development and pro-inflammatory cytokine response in pigs with vaccine-associated enhanced respiratory disease induced by challenge with pandemic (2009) A/H1N1 influenza virus. *Vet. Pathol.* **49**, 900–912 (2012).
8. A. J. Caton, G. G. Brownlee, J. W. Yewdell, W. Gerhard, The antigenic structure of the influenza virus A/PR/8/34 hemagglutinin (H1 subtype). *Cell* **31**, 417–427 (1982).
9. S. Khurana, C. Larkin, S. Verma, M. B. Joshi, J. Fontana, A. C. Steven, L. R. King, J. Manischewitz, W. McCormick, R. K. Gupta, H. Golding, Recombinant HA1 produced in *E. coli* forms functional oligomers and generates strain-specific SRID potency antibodies for pandemic influenza vaccines. *Vaccine* **29**, 5657–5665 (2011).
10. S. Khurana, N. Verma, J. W. Yewdell, A. K. Hilbert, F. Castellino, M. Lattanzi, G. Del Giudice, R. Rappuoli, H. Golding, MF59 adjuvant enhances diversity and affinity of antibody-mediated immune response to pandemic influenza vaccines. *Sci. Transl. Med.* **3**, 85ra48 (2011).
11. S. Khurana, N. Verma, K. R. Talaat, R. A. Karron, H. Golding, Immune response following H1N1pdm09 vaccination: Differences in antibody repertoire and avidity in young adults and elderly populations stratified by age and gender. *J. Infect. Dis.* **205**, 610–620 (2012).
12. N. Verma, M. Dimitrova, D. M. Carter, C. J. Crevar, T. M. Ross, H. Golding, S. Khurana, Influenza virus H1N1pdm09 infections in the young and old: Evidence of greater antibody diversity and affinity for the hemagglutinin globular head domain (HA1 domain) in the elderly than in young adults and children. *J. Virol.* **86**, 5515–5522 (2012).
13. P. A. Bullough, F. M. Hughson, J. J. Skehel, D. C. Wiley, Structure of influenza haemagglutinin at the pH of membrane fusion. *Nature* **371**, 37–43 (1994).
14. L. Zhu, Y. Li, S. Li, H. Li, Z. Qiu, C. Lee, H. Lu, X. Lin, R. Zhao, L. Chen, J. Z. Wu, G. Tang, W. Yang, Inhibition of influenza A virus (H1N1) fusion by benzenesulfonamide derivatives targeting viral hemagglutinin. *PLoS One* **6**, e29120 (2012).
15. W. Hunziker, I. Mellman, Expression of macrophage–lymphocyte Fc receptors in Madin–Darby canine kidney cells: Polarity and transcytosis differ for isoforms with or without coated pit localization domains. *J. Cell Biol.* **109**, 3291–3302 (1989).
16. J. W. Yewdell, W. Gerhard, T. Bachi, Monoclonal anti-hemagglutinin antibodies detect irreversible antigenic alterations that coincide with the acid activation of influenza virus A/PR/834-mediated hemolysis. *J. Virol.* **48**, 239–248 (1983).
17. Y. Ghendon, S. Markushin, H. Heider, S. Melnikov, V. Lotte, Haemagglutinin of influenza A virus is a target for the antiviral effect of Norakin. *J. Gen. Virol.* **67** (Pt. 6), 1115–1122 (1986).
18. U. Kumlin, S. Olofsson, K. Dimock, N. Arnberg, Sialic acid tissue distribution and influenza virus tropism. *Influenza Other Respi. Viruses* **2**, 147–154 (2008).
19. S. G. Van Poucke, J. M. Nicholls, H. J. Nauwynck, K. Van Reeth, Replication of avian, human and swine influenza viruses in porcine respiratory explants and association with sialic acid distribution. *Virol. J.* **7**, 38 (2010).
20. R. K. Nelli, S. V. Kuchipudi, G. A. White, B. B. Perez, S. P. Dunham, K. C. Chang, Comparative distribution of human and avian type sialic acid influenza receptors in the pig. *BMC Vet. Res.* **6**, 4 (2010).

21. R. A. Medina, A. García-Sastre, Influenza A viruses: New research developments. *Nat. Rev. Microbiol.* **9**, 590–603 (2011).
22. R. G. Webster, W. J. Bean, O. T. Gorman, T. M. Chambers, Y. Kawaoka, Evolution and ecology of influenza A viruses. *Microbiol. Rev.* **56**, 152–179 (1992).
23. H. L. Forrest, R. G. Webster, Perspectives on influenza evolution and the role of research. *Anim. Health Res. Rev.* **11**, 3–18 (2010).
24. L. Fairbairn, R. Kapetanovic, D. P. Sester, D. A. Hume, The mononuclear phagocyte system of the pig as a model for understanding human innate immunity and disease. *J. Leukoc. Biol.* **89**, 855–871 (2011).
25. M. M. Swindle, A. Makin, A. J. Herron, F. J. Clubb Jr., K. S. Frazier, Swine as models in biomedical research and toxicology testing. *Vet. Pathol.* **49**, 344–356 (2012).
26. F. Meurens, A. Summerfield, H. Nauwynck, L. Saif, V. Gerdts, The pig: A model for human infectious diseases. *Trends Microbiol.* **20**, 50–57 (2012).
27. D. R. Braucher, J. N. Henningson, C. L. Loving, A. L. Vincent, E. Kim, J. Steitz, A. A. Gambotto, M. E. Kehrli Jr., Intranasal vaccination with replication-defective adenovirus type 5 encoding influenza virus hemagglutinin elicits protective immunity to homologous challenge and partial protection to heterologous challenge in pigs. *Clin. Vaccine Immunol.* **19**, 1722–1729 (2012).
28. M. Throsby, E. van den Brink, M. Jongeneelen, L. L. Poon, P. Alard, L. Cornelissen, A. Bakker, F. Cox, E. van Deventer, Y. Guan, J. Cinatl, J. ter Meulen, I. Lasters, R. Carsetti, M. Peiris, J. de Kruif, J. Goudsmit, Heterosubtypic neutralizing monoclonal antibodies cross-protective against H5N1 and H1N1 recovered from human IgM$^+$ memory B cells. *PLoS One* **3**, e3942 (2008).
29. J. Sui, W. C. Hwang, S. Perez, G. Wei, D. Aird, L. M. Chen, E. Santelli, B. Stec, G. Cadwell, M. Ali, H. Wan, A. Murakami, A. Yammanuru, T. Han, N. J. Cox, L. A. Bankston, R. O. Donis, R. C. Liddington, W. A. Marasco, Structural and functional bases for broad-spectrum neutralization of avian and human influenza A viruses. *Nat. Struct. Mol. Biol.* **16**, 265–273 (2009).
30. D. C. Ekiert, G. Bhabha, M. A. Elsliger, R. H. Friesen, M. Jongeneelen, M. Throsby, J. Goudsmit, I. A. Wilson, Antibody recognition of a highly conserved influenza virus epitope. *Science* **324**, 246–251 (2009).
31. D. Corti, F. Sallusto, A. Lanzavecchia, High throughput cellular screens to interrogate the human T and B cell repertoires. *Curr. Opin. Immunol.* **23**, 430–435 (2011).
32. G. S. Tan, F. Krammer, D. Eggink, A. Kongchanagul, T. M. Moran, P. Palese, A pan-H1 anti-hemagglutinin monoclonal antibody with potent broad-spectrum efficacy in vivo. *J. Virol.* **86**, 6179–6188 (2012).
33. S. Khurana, A. L. Suguitan Jr., Y. Rivera, C. P. Simmons, A. Lanzavecchia, F. Sallusto, J. Manischewitz, L. R. King, K. Subbarao, H. Golding, Antigenic fingerprinting of H5N1 avian influenza using convalescent sera and monoclonal antibodies reveals potential vaccine and diagnostic targets. *PLoS Med.* **6**, e1000049 (2009).
34. S. Khurana, W. Chearwae, F. Castellino, J. Manischewitz, L. R. King, A. Honorkiewicz, M. T. Rock, K. M. Edwards, G. Del Giudice, R. Rappuoli, H. Golding, Vaccines with MF59 adjuvant expand the antibody repertoire to target protective sites of pandemic avian H5N1 influenza virus. *Sci. Transl. Med.* **2**, 15ra5 (2010).
35. A. C. Monsalvo, J. P. Batalle, M. F. Lopez, J. C. Krause, J. Klemenc, J. Z. Hernandez, B. Maskin, J. Bugna, C. Rubinstein, L. Aguilar, L. Dalurzo, R. Libster, V. Savy, E. Baumeister, G. Cabral, J. Font, L. Solari, K. P. Weller, J. Johnson, M. Echavarria, K. M. Edwards, J. D. Chappell, J. E. Crowe Jr., J. V. Williams, G. A. Melendi, F. P. Polack, Severe pandemic 2009 H1N1 influenza disease due to pathogenic immune complexes. *Nat. Med.* **17**, 195–199 (2011).
36. K. K. To, A. J. Zhang, I. F. Hung, T. Xu, W. C. Ip, R. T. Wong, J. C. Ng, J. F. Chan, K. H. Chan, K. Y. Yuen, High titer and avidity of nonneutralizing antibodies against influenza vaccine antigen are associated with severe influenza. *Clin. Vaccine Immunol.* **19**, 1012–1018 (2012).
37. K. K. To, K. H. Chan, I. W. Li, T. Y. Tsang, H. Tse, J. F. Chan, I. F. Hung, S. T. Lai, C. W. Leung, Y. W. Kwan, Y. L. Lau, T. K. Ng, V. C. Cheng, J. S. Peiris, K. Y. Yuen, Viral load in patients infected with pandemic H1N1 2009 influenza A virus. *J. Med. Virol.* **82**, 1–7 (2010).
38. R. Platt, A. L. Vincent, P. C. Gauger, C. L. Loving, E. L. Zanella, K. M. Lager, M. E. Kehrli Jr., K. Kimura, J. A. Roth, Comparison of humoral and cellular immune responses to inactivated swine influenza virus vaccine in weaned pigs. *Vet. Immunol. Immunopathol.* **142**, 252–257 (2011).
39. J. Loebbermann, L. Durant, H. Thornton, C. Johansson, P. J. Openshaw, Defective immunoregulation in RSV vaccine-augmented viral lung disease restored by selective chemoattraction of regulatory T cells. *Proc. Natl. Acad. Sci. U.S.A.* **110**, 2987–2992 (2013).
40. R. Rudraraju, B. G. Jones, R. Sealy, S. L. Surman, J. L. Hurwitz, Respiratory syncytial virus: Current progress in vaccine development. *Viruses* **5**, 577–594 (2013).
41. B. R. Murphy, G. A. Prince, E. E. Walsh, H. W. Kim, R. H. Parrott, V. G. Hemming, W. J. Rodriguez, R. M. Chanock, Dissociation between serum neutralizing and glycoprotein antibody responses of infants and children who received inactivated respiratory syncytial virus vaccine. *J. Clin. Microbiol.* **24**, 197–202 (1986).
42. B. R. Murphy, E. E. Walsh, Formalin-inactivated respiratory syncytial virus vaccine induces antibodies to the fusion glycoprotein that are deficient in fusion-inhibiting activity. *J. Clin. Microbiol.* **26**, 1595–1597 (1988).
43. M. F. Delgado, S. Coviello, A. C. Monsalvo, G. A. Melendi, J. Z. Hernandez, J. P. Batalle, L. Diaz, A. Trento, H. Y. Chang, W. Mitzner, J. Ravetch, J. A. Melero, P. M. Irusta, F. P. Polack, Lack of antibody affinity maturation due to poor Toll-like receptor stimulation leads to enhanced respiratory syncytial virus disease. *Nat. Med.* **15**, 34–41 (2009).
44. C. A. Shaw, G. Otten, A. Wack, G. A. Palmer, C. W. Mandl, M. L. Mbow, N. Valiante, P. R. Dormitzer, Antibody affinity maturation and respiratory syncytial virus disease. *Nat. Med.* **15**, 725 (2009).
45. P. G. Halbur, P. S. Paul, M. L. Frey, J. Landgraf, K. Eernisse, X. J. Meng, M. A. Lum, J. J. Andrews, J. A. Rathje, Comparison of the pathogenicity of two US porcine reproductive and respiratory syndrome virus isolates with that of the Lelystad virus. *Vet. Pathol.* **32**, 648–660 (1995).
46. K. Tamura, D. Peterson, N. Peterson, G. Stecher, M. Nei, S. Kumar, MEGA5: Molecular evolutionary genetics analysis using maximum likelihood, evolutionary distance, and maximum parsimony methods. *Mol. Biol. Evol.* **28**, 2731–2739 (2011).

Acknowledgments: We thank J. Yewdell, M. Eichelberger, and C. Weiss for their thorough review and insightful comments. We also thank M. Harland and G. Nordholm for technical assistance and J. Huegel, J. Crabtree, and T. Standley for assistance with animal studies. **Funding:** Funding was provided by Agricultural Research Service, U.S. Department of Agriculture (USDA). Mention of trade names or commercial products in this article is solely for the purpose of providing specific information and does not imply recommendation or endorsement by the USDA. USDA is an equal opportunity provider and employer. **Author contributions:** S.K., C.L.L., A.L.V., and H.G. designed and performed the experiments, analyzed the data, and wrote and edited the paper. J.M., L.R.K., J.H., and P.C.G. performed the experiments, analyzed the data, and read the paper. **Competing interests:** The authors declare that they have no competing interests.

Submitted 6 April 2013
Accepted 26 June 2013
Published 28 August 2013
10.1126/scitranslmed.3006366

Citation: S. Khurana, C. L. Loving, J. Manischewitz, L. R. King, P. C. Gauger, J. Henningson, A. L. Vincent, H. Golding, Vaccine-induced anti-HA2 antibodies promote virus fusion and enhance influenza virus respiratory disease. *Sci. Transl. Med.* **5**, 200ra114 (2013).